

# PHOTON ECHOES OF MOLECULAR PHOTOASSOCIATION\*

Alexander G.Rudavets<sup>† 1</sup>

<sup>1</sup>*Moscow Institute of Physics and Technology, 141700 Dolgoprudny, Russia*

Alexander M.Dykhne<sup>1,2</sup>

<sup>2</sup>*TRINITI, 142092 Troitsk, Russia*

## Abstract

Revivals of optical coherence of molecular photoassociation driven by two ultrashort laser pulses are addressed in the Condon approach. Based on textbook examples and numerical simulation of KrF excimer molecules, a prediction is made about an existence of photon echo on free-bound transitions. Delayed rise and fall of nonlinear polarization in the half-collisions are to be resulted from the resonant quantum states interference whether it be in gas, liquid or solid phases.

**Keywords:** Photon echo, molecular photoassociation, femtosecond spectroscopy

## 1. Introduction

At present, the photoassociation spectroscopy (PAS) of atoms colliding along the ground state potential and interacting with photons to produce molecular dimers (through the inverse predissociation) has attracted a great deal of attentions<sup>1-7</sup>. This technique, as applied in conventional continuous wave<sup>5,16</sup> (CW) and femtosecond<sup>1</sup> regimes, permits a determination of the rovibrational levels, hyperfine structure, scattering lengths and/or dynamics of bond formation that can be derived with an unprecedented accuracy. To assess the primary processes of harpooning reactions<sup>2</sup>, photoassociative and the Penning ionizations<sup>3</sup>, relaxation of the van der Waals complexes<sup>4</sup> in liquids and quantum gases in optical traps, the PAS is ideally suited. The review of earlier devel-

---

\*Proceedings of SPIE Vol.3734, 86-95 (1999)

<sup>†</sup>address for correspondences: Arudavets@mics.msu.su

opments, which have been collected under the rubric of chemical reactions in transition spectroscopy, can be found in <sup>6</sup>. The most recent innovation to the CW PAS is investigation of Bose's state of the cold atoms<sup>7</sup> in which a loss of coherence can be controlled through the laser assisted binary collisions.

One would naively claim that the femtosecond PAS is not quite sensitive as the resonant CW schemes, since only a low number of atoms distributed randomly in close proximity during ultrashort pulses may contribute to the coherent bonding. However, the shorter impulse, the wider its spectrum, the more the free-bound transitions involved. An example is found in photoinduced harpooning reactions <sup>8</sup> in which according to the M. Polanyi the attacking open shell atom tosses out its valence electron, then hooks the closed shell atom and hauls it in with the Coulomb force even at a range of hundreds Angstroms<sup>1</sup>. This reaction endowed with separation of degrees of freedom into nuclear and electronic coordinates controlled by the femtosecond optical pulses may have a high quantum yield.

It is straightforward to extend the femtosecond PAS to address the four wave mixing geometry or its two or three wave realizations. This makes it possible to investigate the nonlinear optical effects those are no longer observable in the weak fields. Such as a photon echo photoassociation which is counterpart of the photon echo of photodissociation. A theoretical description of the latter is only being reported by us <sup>9,10</sup> in context of the wave packet engineering. It is evident now, that a well matched spreading and squeezing of the vibrational wave packets are called for the desired optical properties of molecular samples. So that the quantum control in the weak field regime requires a complicated pulse shaping <sup>11</sup>. While "spontaneous" coherence, i.e., a photon echo, is obtained through a more strong, short and transform limited (non chirped) fields that enables one to automate the wave packet preparation on the free-bound transitions.

The transients having the entanglement of discrete levels and continuum usually result in a decay <sup>12</sup>. The quantum transition amplitudes may decrease depending on the contribution of the molecular repulsion or quantum dispersion. In the frequency domain, the resonant coupling is accompanied by the inhomogeneous broadening (dephasing) of the Franck-Condon transitions. If the latter dominates over an irreversible relaxation in multi-channel (chemical) collisions, spontaneous emission, the photon echo can be harvested as for the bound-bound transitions <sup>13</sup>.

To make this point a bit clear, we follow the next plan. In Sec.2 the Condon model of femtosecond PAS is analyzed. We relate the delayed transients to the wave packet interference residing in molecular continuum after the second im-

---

<sup>1</sup>The long-range of the reaction increasingly grows at low temperature

pulse. Analytical expressions are derived for the  $\chi^{(3)}$  polarization induced by 2  $\delta$ -like impulses. A singularity of  $\chi^{(3)}$  is identified with an infinite region of the Franck-Condon transitions simultaneously involved. For the realistic field shapes this trait is eliminated. The PAS is particularly appealing for the investigating excitations of the rare gas halides, for which the electronic ground states are dissociating. This system is of use as an active media of the high-power lasers<sup>2</sup> and photon echo of photoassociation might deliver a valuable information on timescales of excited molecular states in the lasing. Specifically, the relevant model of molecular dynamics of the krypton fluoride KrF(B) excimer is simulated in Sec.3, where we consider a photoinduced harpooning reaction of interacting Kr cations and F anions created at thermal conditions. To avoid the Condon reflection principle, which overestimates contribution of turning points and disregards oscillatory tails of the wave functions, the B-X transition (at 248 nm) is treated in the globally uniform approach. The Wigner representation gives an insight into why the photon echoes of photoassociation exist from the kinematical point of view. Section 4 concludes.

## 2. Condon Model

Strictly speaking, 'ab-initio' approach to PAS necessitates a many-body field theory of interacting matter-light species. However, any more rigorous treatment of the photoassisted reactions beyond the Born-Oppenheimer strategy faces sophisticated mathematical problems of exclusion of extra degrees of freedoms and transitions between multidimensional surfaces. It is not surprising, then, that a generic model with simplified potential curves, in which the bound-free transitions occur in one-body treatment, has been introduced at the dawn of the age of quantum mechanics<sup>14</sup>. Herein, a separation of degrees of freedom gives the paradigm of application of the Franck-Condon principle asserting that for a time of electron transfer, the coordinates and momenta of nuclei do not vary because of the large difference between the electronic and nuclear masses. Molecular dynamics is governed by the Hamiltonian operators:

$$\hat{H}_b = \hat{T}_{kin} + \hat{V}_b; \quad \hat{H}_f = \hat{T}_{kin} + \hat{V}_f,$$

where  $\hat{T}_{kin}$  is the operator of kinetic energy of relative motion in the motionless center mass of a molecule and the Doppler's shift of frequency is disregarded as marginal. Initially, atoms collide along the ground electronic term with constant interatomic interaction  $\hat{V}_f = 0$ . The excited electronic curve can be presented by the potential  $\hat{V}_b = \omega_0 + \Omega^2 x^2 / 2$  with understanding that the actual curves are deflected of the parabolic well at longer and shorter distances from

---

<sup>2</sup>Europe's largest KrF excimer laser "TITANIA" (<http://www.clf.rl.ac.uk/index.html>) has an output of  $10^{19} \text{W/cm}^2$  and pulses duration 350 fs

its equilibrium position. The model potential has merit of being exactly solved best serving for our methodological purpose. We have chosen the test example of oscillatory motion with frequency  $\Omega$  as a vehicle with which to demonstrate general aspects of photoassociation. Without restricting the generality, an effective mass of molecule equals unit. The electronic states are coupled by the electric dipole interaction  $\hat{V}_{bf} = \hat{\mu}E(t)$ , where the laser impulses have the slow envelopes  $E(t)$  and fast optical frequency  $\omega_0$ . The envelope differs from zero only for the moments of photon impacts.

With the rotating wave approximation, the Schrödinger equation for the bound states  $|\psi_b\rangle$  and scattering states  $|\psi_f\rangle$  can be written in the notation of Dirac as

$$\begin{aligned} i\hbar|\dot{\psi}_b\rangle &= \hat{H}_b|\psi_b\rangle + \hat{V}_{bf}|\psi_f\rangle \\ i\hbar|\dot{\psi}_f\rangle &= \hat{H}_f|\psi_f\rangle + \hat{V}_{fb}|\psi_b\rangle. \end{aligned} \quad (1)$$

In order to have general formalism capable of dealing with both bound and scattering states, we employ the momentum representation. A crucial assumption is made that our system has a very large box volume  $V$ . The energy spectrum of atoms forming the plane waves is bound to be quasi-continuous in the box. It is required of the initial quantum conditions  $\langle p|\psi_f(0)\rangle = \psi_f^0(p)$  that the box wave functions possess the property of random phases. This requirement corresponds to the "molecular chaos" with the canonical Gibbs thermal distribution in the atomic ensemble:

$$\langle \psi_f^0(p_1)\psi_f^0(p) \rangle_{ave} = Z^{-1} e^{-\beta H_f(p)/\hbar} \delta(p - p_1),$$

where  $\beta$  is the inverse temperature,  $Z$  is the statistical sum. The box normalization (a molecule per the box volume) is implied. The quasi-continuous states correlate initially only with the coincident momenta giving the Gibbs density, while the bound molecular states are empty  $|\psi_b(0)\rangle = 0$  before the laser excitation.

The resonant states between the laser impulses are governed by the molecular evolution operators

$$\begin{aligned} |\psi_b(t)\rangle &= e^{-it\hat{H}_b/\hbar} |\psi_b(0)\rangle \\ |\psi_f(t)\rangle &= e^{-it\hat{H}_f/\hbar} |\psi_f(0)\rangle, \end{aligned} \quad (2)$$

where the momentum representation can be used to arrive at the matrix elements

$$\begin{aligned} \langle p|e^{-i\frac{t\hat{H}_f}{\hbar}}|p_1\rangle &= e^{-itp^2/2\hbar} \delta(p - p_1) \\ \langle p|e^{-i\frac{t\hat{H}_b}{\hbar}}|p_1\rangle &= \frac{e^{i((p^2+p_1^2)\cos(\Omega t)-2pp_1)/(2\hbar\Omega\sin(\Omega t))}}{\sqrt{2i\hbar\Omega\pi\sin(\Omega t)}}. \end{aligned} \quad (3)$$

The laser field couples the resonant electronic states  $|\psi_b\rangle$  and  $|\psi_f\rangle$  and to prepare their mixing in the limit of a weak, short impulse according to eq. (1)

$$\begin{aligned} |\psi_b(\tau)\rangle &= -i\theta|\psi_f^0\rangle \\ |\psi_f(\tau)\rangle &= |\psi_f^0\rangle - i\theta|\psi_b(\tau)\rangle, \end{aligned} \quad (4)$$

where zero time  $t = 0$  corresponds to the beginning of an ultrashort pulse of the duration  $\tau$ , so that  $\theta = \tau\mu \cdot E/\hbar \ll \pi$  is the pulse area.

Let us consider an idealization of the  $\delta$ - like impulses. The Franck-Condon principle ensures the intact positions and momenta of the wave packets on the resonant electronic terms during the laser field action. The optical polarization of the system is found by calculating the dipole moment  $\mu$  in the Condon approximation in which a total span of Franck-Condon region of free-bound transition includes the (infinite) box  $V$ , whilst the relative electronic transition moment, i.e., the dipole operator  $\hat{\mu}$  is independent of a position of atoms in the box:

$$\langle \hat{\mu}(t) \rangle_{ave} = \mu \langle \langle \psi_f(t) | \psi_b(t) \rangle \rangle_{ave}. \quad (5)$$

The free decay of the optical polarization after the first laser impulse follows the time dependent Fermi golden rule:

$$\langle \hat{\mu}^{(1)} \rangle_{ave} = -i\mu\theta \text{Tr}[e^{-it\hat{H}_b/\hbar} e^{i(t+i\beta)\hat{H}_f/\hbar}] / Z = -i\mu\theta K^{(1)}(t), \quad (6)$$

where the identity relation  $\hat{I} = \int dp |p\rangle \langle p|$  and the matrix elements of Eq. (3) are applied for the trace calculation

$$\begin{aligned} K^{(1)}(t) &= Z^{-1} [2\pi\hbar\Omega \sin(\Omega t)]^{-1/2} \int dp e^{i[\beta + t + tg(\Omega t/2)/\Omega]p^2/2\hbar} = \\ &= Z^{-1} [\cos(W_{decay}(t)) - 1]^{-1/2}. \end{aligned} \quad (7)$$

The kernel  $K^{(1)}$  is determined by a "hyperbolic" rotation on complex angle  $W(t)$  given by:

$$\cos(W_{decay}(t)) = \cos(\Omega t) + 0.5\Omega(i\beta + t)\sin(\Omega t), \quad (8)$$

The hyperbolic rotation is inspired by the dynamical symmetry group  $SU(1,1)$  responsible for the phase and amplitude modulation of average dipole moment. In frequency domain, the hyperbolic rotation gives rise in inhomogeneous broadening of spectral lines of free-bound transitions<sup>15</sup>.

The free-bound transition amplitude  $K^{(1)}(t)$  has a time-integrable singularity of the order  $1/\sqrt{t}$ . Notice that this kernel is resulted from an unbounded spectrum of the simultaneously driven resonant transitions induced by the  $\delta$ -pulse. This artifact of the polarization singularity can be corrected whether by a dipole moment cutoff that leads us beyond the Condon approximation

and/or frequency limited spectrum of the excitation field. However, being the  $\mu$  cutoff length dependent, it becomes tedious for the analytical analysis. The thermalization and internal molecular interference add to the complexity of the problem. This is the case of femtosecond PAS. The nonlinear optical polarization depends also on the multi-dimensional convolutions of the actual field envelopes with the singular kernels induced by the  $\delta$  fields. Their nonlinear combinations provide another vectors of directional coherence along which the echo signals are to be observed. We shall set these problems aside for sake of simplicity to treat molecular photoassociation in the  $\delta$ -pulse limit and focusing on collinear geometry of incident electromagnetic wave vectors. Suggesting that these two  $\delta$ -pulses operate having the inter-pulse delay  $T$ , we find the mixing bound and free states as

$$\begin{aligned} |\psi_f(T)\rangle &= [e^{-iT\hat{H}_f/\hbar} - \theta_1\theta_2e^{-iT\hat{H}_b/\hbar}]\psi_f^0, \\ |\psi_b(T)\rangle &= -i\theta_2e^{-iT\hat{H}_f/\hbar}\psi_f^0, \end{aligned} \quad (9)$$

where the initial state  $|\psi_f^0\rangle$  belongs to the Gibbs distribution of collision pairs. By  $\theta_1$  and  $\theta_2$  we denote the areas of the first and the second laser impulses respectively. These pulses govern a quantum superposition of the states

$$\begin{aligned} |\psi_f(t)\rangle &= [e^{-it\hat{H}_f/\hbar} - \theta_1\theta_2e^{-i(t-T)\hat{H}_f/\hbar}e^{-iT\hat{H}_b/\hbar}]\psi_f^0 \\ &= |\psi_f^0(t)\rangle - \theta_1\theta_2|\bar{\psi}_f^0(t)\rangle, \\ |\psi_b(t)\rangle &= -i\theta_2e^{-i(t-T)\hat{H}_b/\hbar}e^{-iT\hat{H}_f/\hbar}\psi_f^0 \\ &= -i\theta_2|\bar{\psi}_b(t)\rangle, \end{aligned} \quad (10)$$

in which the normalized state vectors  $|\bar{\psi}_b(t)\rangle, |\bar{\psi}_f(t)\rangle$  entering Eq.(10) with the coefficients proportional to  $\theta_2$  and  $\theta_1\theta_2$  yield a dominant contribution to the delayed transition amplitudes. We call these vectors as the "propagating" states<sup>10</sup>. The free-bound transients are presented by a series of the propagation operators each of them being responsible for an adiabatic step along the molecular curves. Therefore, a first nonlinear correction to the dipole moment averaged over the Gibbs distribution can be cast as

$$\begin{aligned} \langle \hat{\mu}^{(3)} \rangle_{ave} &= i\mu\theta_1\theta_2^2K^{(3)}(t), \\ K^{(3)}(t) &= Tr[e^{i\frac{(T-t)\hat{H}_b}{\hbar}}e^{i\frac{(t-T)\hat{H}_f}{\hbar}}e^{-i\frac{T\hat{H}_b}{\hbar}}e^{-\frac{(\beta-iT)\hat{H}_f}{\hbar}}]/Z. \end{aligned} \quad (11)$$

Using the momentum representation of the propagation operators and performing this 2-d Gauss integration over momenta in the matrix elements Eqs.(3,13), we obtain a characteristic function

$$K^{(3)}(t) = Z^{-1}[\cos(W_{echo}(t)) - 1]^{-1/2}, \quad (12)$$

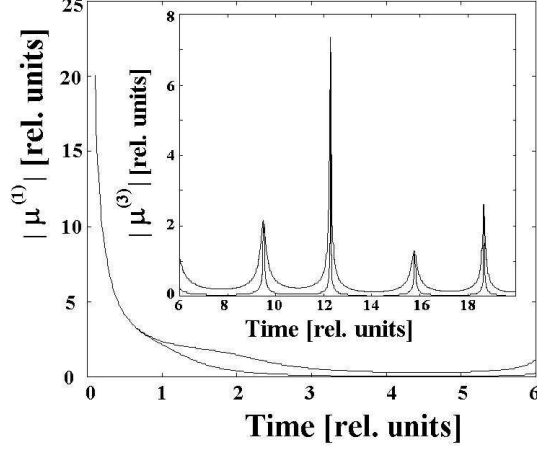


Figure 1 The free radiation decay and echo transients in the Condon model. The higher temperature, the faster the decay and the sharper the photon echo peaks. This behaviour is illustrated by two curves at inverse temperature  $\beta = 1/\Omega$  and  $\beta = 1/5\Omega$ . Inset displays the  $\mu^{(3)}$  dipole moment arising on free-bound transition following the second ultrashort impulse which fires with delay  $T \approx 2\pi/\Omega$  matching molecular period. Use of normalized impulse areas  $\theta_{1,2} = 1$  and frequency  $\Omega = 1$  is made here.

in which a hyperbolic rotation owing to the 2-pulse interaction is

$$\begin{aligned} \cos(W_{echo}(t)) &= \cos(\Omega\bar{t}) + 0.5\Omega((\bar{t} + i\beta)\sin(\Omega\bar{t}) \\ &+ \Omega(\bar{t} + T)(T - i\beta)\sin(\Omega(\bar{t} + T))\sin(\Omega T)), \end{aligned} \quad (13)$$

being conveniently expressed through the shifted time  $\bar{t} = t - 2T$ .

For the weak field regime the resonant coupling of continuum and bound wave functions in the Franck-Condon region is determined by the time dependent Fermi golden rule as shown in Fig. 1. A monotonic decay of the Franck-Condon factors will no longer be valid at a low temperature, e.g. at inverse temperature  $\beta = 1/\Omega$  corresponding to one vibrational quantum. The reason has to do with the quantum dispersion which alone cannot destroy coherence. Molecular repulsion for inclined potential curves or predissociation would afford exponential decay<sup>12</sup>. But even in this instance, a net constructive or destructive interference of two wave packets prepared by the pump and delayed impulses occurring at or near multiples of the vibrational period might result in the revivals of coherence. The transition amplitude spikes reflect the return of the vibrational wave packet on the attractive potential curve.

To consider the echo effect in the weak field regime we derived the  $\mu^{(3)}$ -polarization from Eqs.(11-13). In the Condon model, the transition amplitudes between the propagating states are obtained explicitly as a function of time and an average polarization is plotted in inset in Fig.1. The echo signal itself consists of a number of short peaks most prominent when a delay  $T$  is close to multiple of the vibrational period ( $T \approx T_{vib} = 2\pi/\Omega$ ). The Eq.(13) determines the positions of the "spontaneous" revivals near  $t = nT, (n + 1/2)T$   $n = 1, 2, \dots$ . In the occasion  $|\sin(\Omega T)| \ll 1$  and  $(\Omega T \sin(\Omega T))^2 > 1$ , we easily see that the half width at a half maximum (HWHM) at  $t = 2T$  is estimated from

Eq.(13) as

$$\tau_{echo} \approx \beta/\Omega T. \quad (14)$$

This simple expression can be understood as a time taken by a classical particle to move the thermal de-Broglie wavelength  $r_0 \propto \sqrt{\beta}$  with velocity  $v = \Omega \langle R \rangle_{ave}$  depending directly on the correlation radius  $\langle R \rangle_{ave}$  of the propagating state in the continuum of states,

$$\langle R(2T) \rangle_{ave} = \langle \langle \bar{\psi}_f(2T) | \hat{R} | \bar{\psi}_f(2T) \rangle \rangle_{ave} \propto T v_0,$$

where  $v_0 \propto 1/\sqrt{\beta}$  is the thermal velocity of atoms. So that, we obtain the correlation time  $\tau_{cor} = r_0/Tv_0 = \beta/\Omega T$ , which matches Eq.(14) for HWHM and has to play a key role in determining the nonlinear polarization peaks. What this means is the validity of kinematical argumentation based on the quasiclassical transport theory allowing us to justify the echo of photoassociation just as the photon echo of molecular photodissociation<sup>10</sup>. It is appropriate to recall that in the latter, the ground molecular wave function forms a wave packet of the receding atoms following first impulse. Atomic distribution acquires a stretched elliptic shape in the phase space formed by the coordinates and velocities. The ellipse is strongly squeezed in the transversal direction by virtue of "free" propagation. However, the total phase space volume (according to the Liouville theorem) persists. Being driven back by the second impulse, the wave packet replica settles in the binding term as a non stationary state.

For the harmonic model, the ellipse rotates as a hole at the vibrational frequency. In addition, the replica of the initial state, which was preserved after the first impulse, repeats the evolution of the wave packet in the molecular continuum. The transition amplitude  $|K^{(3)}|^2$  strongly depends on the interference between the quantum-mechanical paths of the wave packets driven in tandem. The last manifests in squeezing of the photon echo peaks inversely quadratic of the delay  $T$ :

$$\tau_{echo} = \tau_{decay}/((\Omega T)^2 + 1), \quad (15)$$

where  $\tau_{decay}$  is the time of free radiation decay depending on molecular curves and temperature. It equals a molecular radius  $a$  divided by typical velocity of receding atoms in the phase space. The longer the inter-pulse delay  $T$ , the larger the squeezing of molecular states, the larger the correlation radius of receding atoms, and the faster decay of the Franck-Condon overlapping. This implies, that the wave packet moving on the smaller ellipse diameter  $a$  varying as  $1/\Omega T$  has to move it with velocity  $v$  which grows directly  $\Omega T$  (proportional to the correlation radius). The overlap time is given by the ratio  $a/v$  to yield the mentioned trend  $\tau_{echo} \propto (\Omega T)^{-2}$ .

The same reason holds true for the photon echo of photoassociation. But its duration features its inverse power of  $T$ . This is because only a propagating state in the continuum is being squeezed after the second impulse as a function



of inter-pulse delay. The difference between the echo scaling laws for the photodissociation and photoassociation is founded on the fact, that, in the former, both wave packets evolved on the binding term and in the continuum X-states are squeezed. Also the  $\mu^{(3)}$ -polarization has a maximum peak near  $t = 2T$ . Our analysis indicates that the HWHM increasingly decreases with the temperature. Besides, at the delay time exactly matching the oscillatory period  $2\pi/\Omega$ , the amplitude of spontaneous revivals may appear to diverge at points  $t = 2T$ . Fortunately, this divergence rules out in the  $\mu^{(3)}$  polarization controlled by the realistic laser field which shape differs from the  $\delta$ -like envelopes.

The theory of this phenomenon is best clarified in the phase space of the system. The free-bound transitions are characterized by the distribution of the collisional pairs over their electronic excitations, internuclear separations and velocities. Therefore an uniform representation for the scattering states, those are quasiclassical in their nature, may be helpful. Just as for the photodissociation picture, the molecular dynamics can be visualized for the Wigner distribution functions. For the thermal atoms, the Wigner map has the shape of infinite strip along the coordinate axis. The strip width in the transversal direction is equal to the thermal de-Broglie wavelength.

The first impulse conveys the collisional pair to the binding electronic B-term. The replica of the thermal Wigner distribution sets here. After that, the atoms oscillate between the turning points. This corresponds to the strip distribution in phase space which rotates at the harmonic frequency. The second impulse does the same with the remaining portion of colliding atoms. In addition, it simultaneously promotes the rotated strip to the continuum, where the latter starts to spread along the coordinate axis. The spreading distribution squeezes in transversal direction. It is apparent, that their overlap sharply rises and falls, when the adjacent Wigner maps cross each other. If the maps turn out parallel, a total span of the induced free-bound transitions includes an infinite volume of our simplistic model enabling the Franck-Condon factor to diverge.

### 3. Wigner Functions of Photoassociation of Kr-F Collisional Pairs

Consider the product of the density matrices of the ground and excited electronic states. The time-delayed nonvanishing overlap of the states in phase space would signature an existence of photon echo of photoassociation. For ultrashort pulses, the propagating states contribute to the delayed transients. Then, the density matrices  $\hat{\rho}_b = \langle |\psi_b\rangle\langle\psi_b| \rangle_{ave}$  and  $\hat{\rho}_f = \langle |\psi_f\rangle\langle\psi_f| \rangle_{ave}$  are related to the Wigner distribution function  $W_\alpha(p, q)$  via the Fourier transform in the coordinate space

$$W_\alpha(p, q) = (2\pi)^{-1} \int dr e^{ipr} \langle \langle q - r/2 | \psi_\alpha \rangle \langle \psi_\alpha | q + r/2 \rangle \rangle_{ave}, \quad \alpha = b, f. \quad (16)$$

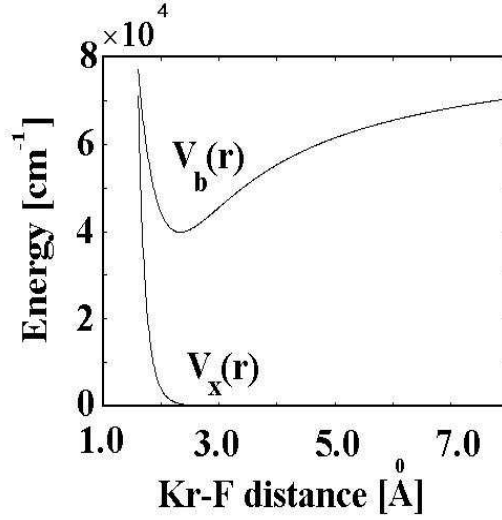


Figure 2 Interaction between Kr cation and F anion is described by the truncated Ritner potential<sup>16</sup>,  $V_b(r) = a + be^{-\gamma r} - c_1 r^{-1} - c_4 r^{-4}$ , where  $r$  is the Kr-F distance,  $a = 85510 [cm^{-1}]$  is the separated ion limit,  $\gamma = 2.94 [A^{-1}]$  and  $b = 1.01 \times 10^7 [cm^{-1}]$  are the constants of electron shells exchange repulsion,  $c_1 = 2.19 \times 10^5 [cm^{-1} A]$  and  $c_4 = 1.7 \times 10^5 [cm^{-1} A^4]$  are the parameters of Coulombic and ion-quadrupole interactions respectively for the  $B\Sigma_{1/2}^+$  state. For the ground  $X\Sigma_{1/2}^+$  state, the interaction potential is assumed to be purely repulsive:  $V_x(r) = c_{13} r^{-13}$ , where  $c_{13} = 3.2 \times 10^7 [cm^{-1} A^{13}]$ .

The overlap of the Wigner distribution functions in the phase-space is expressed as

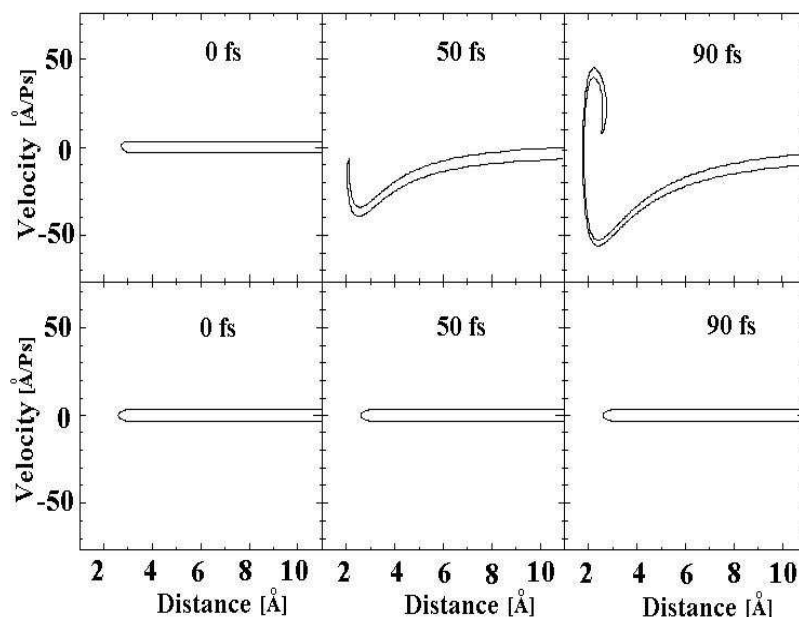
$$Tr[\hat{\rho}_b \hat{\rho}_f] = \iint dpdq W_b(p, q) W_f(p, q). \quad (17)$$

In our simple model, the quasiclassical functions  $W_\alpha(p, q)$  follow the Liouville transport equations

$$\frac{\partial W_\alpha}{\partial t} + p \frac{\partial W_\alpha}{\partial q} - \frac{\partial V_\alpha}{\partial q} \frac{\partial W_\alpha}{\partial p} = 0, \quad (18)$$

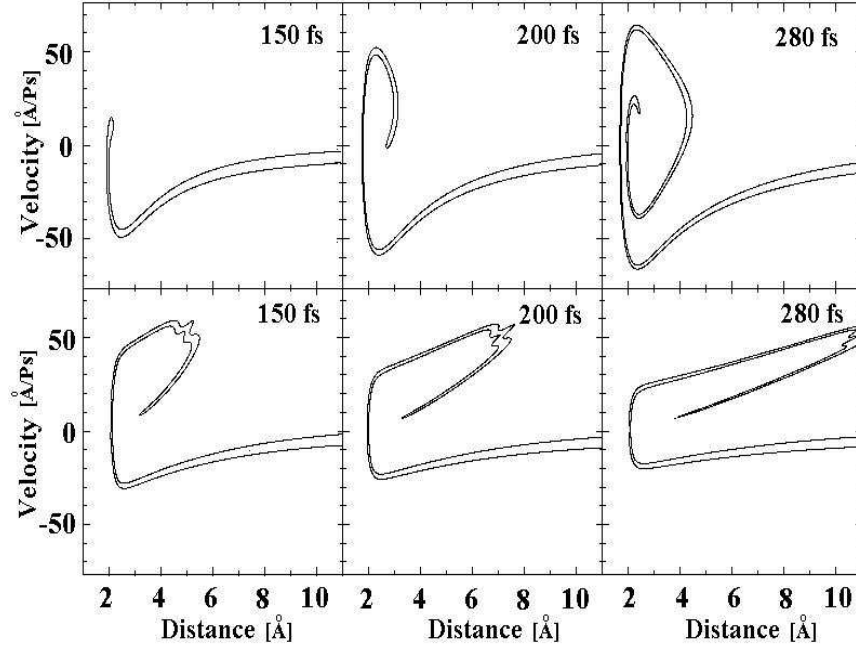
with an accuracy of  $\hbar^2$  independent of the model potentials under study. This approach guarantees an uniform treatment of molecular dynamics even though a major contribution to the overlap integral is accumulated near the turning points, where the standard quasiclassical theory fails. We take an advantage of the Wigner representation to calculate the matrix density overlap of Kr( $4p^6 S_0$ )-F( $2p^5 \ ^2P$ ) photoassisted collisions along X- and B-molecular terms shown in Fig.2. Applying the classical dynamic routines to colliding Kr and F atoms, we directly obtain the Wigner density functions of photoassociation. The  $\delta$ -like envelopes of laser fields allow us to deal just with the propagating states density. In Fig. 3 we display the contour maps calculated from the transport equation Eq. (17). The thermal atoms occupy the half-strip terminating in a short distance due to the strong exchange repulsion on the covalent X-term.

Figure 3. The Wigner contour map of the density of KrF excimer molecules immediately following an ultrashort pulse at 0 fs, 50 fs and 90 fs. Upper panels show evolution of the Wigner functions due to a harpooning reaction on the ionic B-curve. Lower panels show the thermal distribution of the colliding atoms along the covalent X-curve. The contour lines are taken at half maximum height of the Wigner's functions



The energy gap between the ground covalent state and bottom of the ionic B-term is in range of 248 nm wavelength resonant to the laser pulse frequency. The Wigner maps in the upper row in Fig. 3 present the evolution of the thermal distribution of the X-states distorted by the first  $\delta$ -pulse that resonantly drives them to ionic B-states. Then, the F anions and Kr cations are attracted together due to the joint action of the Coulomb force and induced ion-quadrupole interactions. In the harpooning reaction, the Wigner map of the thermal atoms curves forming a hook and then a spiral structure in the phase space. The spiral step is conditioned by the potential anharmonicity. For the pure harmonic model, a rotation of the initial strip as a hole at the oscillatory frequency takes place. The Wigner maps of the propagating X,B-states created by the pulse pair are shown in Fig. 4. We take the inter-pulse delay equal to about a period (90 fs) of molecular vibration in the bottom of B-state. The second impulse transports the Wigner's B-state distribution partially back to continuum, as it is, conserving its spiral shape. The spiral branches are spreading on the covalent X-curve and simultaneously squeezing in the momentum direction. In

Figure 4. The Wigner distribution functions of KrF excimer created by the impulse pair. The interpulse delay is equal to 90 fs i.e. about one molecular period. The Wigner maps are drawn at 150 fs, 200 fs and 280 fs. Upper panels present the harpooning reaction in the ionic B-states. Lower panels show the spreading photofragments in covalent X-state.

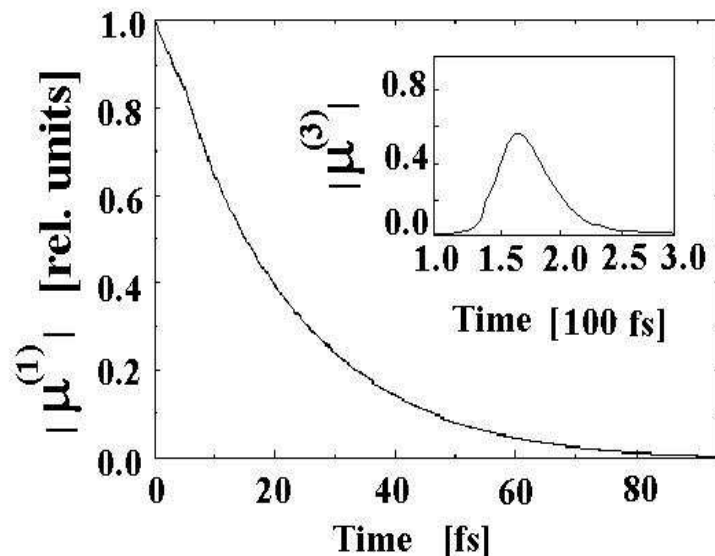


addition, its optical field might induce a harpooning reaction by producing a collisional pair of cation Kr and anion F. The Wigner distribution on their B-binding term repeats the evolution following the first impulse. In Fig. 5 we display the overlap of the molecular densities in the phase space as a function of time. The overlap of the Wigner's distributions of the X and B -states quickly tends to zero. The decay time after the first impulse can be evaluated as a width at the half maximum height of the integral Eq.(17). This time is about 20 fs long that conforms the estimate based on the classical mechanics. Doing so, consider a particle moving with a thermal velocity in the covalent X-state. Its wave packet is transported to the binding B-term via a vertical Franck-Condon's transitions. Then, it needs the time:

$$\tau_{decay} \approx \int_{R_{in}}^{R_{out}} dr/v_b(r) \quad (19)$$

to destroy an alignment of the Wigner's distributions while the wave packet travels between the turning points in the quantum well. The turning points  $R_{in} \approx 2.15\text{\AA}$  and  $R_{out} \approx 2.65\text{\AA}$  are determined by the thermal energy

Figure 5. The free radiation decay and photon echo of molecular photoassociation of KrF. The HWHM of  $\mu^{(1)}$  polarization is about 20 fs. The relevant  $\mu^{(3)}$  polarization created by two  $\delta$ -like laser fields having normalized pulse areas  $\theta_{1,2} = 1$  and inter-pulse delay 90 fs is shown in inset.



$E_{ther} = 100 [cm^{-1}]$  of collision pairs of Kr and F atoms. The wave packet loses its momentum correlation with nascent replica of X state for time its journey between the turning points. Our first rough estimate of about 40 fs is obtained by substituting to Eq.(19) the velocity:  $v_b(R) = (2(E_{ther} - V_b(R))/M)^{1/2}$ , and by taking the numerical values of the reduced mass  $M \approx 15.5$  of the KrF molecule. Inset also shows the rise and fall of the overlaps of the Wigner's distributions after the second ultrashort pulse. This occurs at twice time-delay, when the hook map crosses the spiral branches of the X-state distribution. Our numerical calculation indicates, that the photon echo signal is rather robust with respect to a small deviations of the inter-pulse delay from the gating conditions  $T = T_{vib}$ . This robustness can be attributed to anharmonicity of the KrF(B) potential.

#### 4. Conclusions

We have demonstrated how the ultrashort pulses can reverse the natural tendency of the nonlinear optical transients to decay in photoassisted half-collisions. The photon echo of molecular photoassociation presents a paradigm of the coherent self-organization in optics. This occurs in the continuum states initially residing in the Gibbs equilibrium ensemble. The photoassociation is

followed by the delayed photodissociation giving rise the correlation radius of propagating states to grow proportionally as the inter-pulse time-delay. The latter results in a long lived transient complex. Then, the echo signals manifests on the free-bound transitions following the free radiation decay that is dictated by the resonant coupling probability in accordance with the time dependent Fermi golden rule. This delayed coherence is accounted for by the inverse predissociation amounting to phenomena conceptually identical with the interference stabilization of atoms (molecules) in the strong ionizing (dissociating) laser fields.

The femtosecond coherence of the laser assisted collisions is formed on the molecular nano-scales and can be observed in optically thin samples. This effect might provide a way to make a compact light compressor without limitations imposed by the self-modulation effects in the optical wave-guides. From the spectroscopic point of view, the photon echo of photoassociation provides for unique data on the fly during the binary half-collisions. The echo spikes splitting can exhibit an inhomogeneous broadening inherent to the distribution of guest atoms in host solid with the sub-wavelength resolution up to Angstrom's scale. This opens up a possibility to trace the migration of open-shell atoms in rare gas matrices and cage exit. Kindred phenomena might be studied by molecular dynamics simulations<sup>17</sup> to provide a new avenue for the echo spectroscopy in solids and liquids.

In brief, therein our major aim was not a quantitative agreement with an experiment, but to broadly predict the general aspects of the photon echo of photoassociation and to delineate those its features which depend on inter-pulse delay of laser pumping, molecular potentials and temperature of sample. The echo scheme has a merit to automate the wave packet preparation making it a quite favorable for a practical design, where the pulse shaping is not necessary. It is important to stress a geometrical aspect of the effect, in which the directional vector  $\vec{k}_1 - 2\vec{k}_2$  of the echo coherence is distinguished from the incident wave vectors  $\vec{k}_1$  and  $\vec{k}_2$  of the pump and delayed fields. This offers a convenient experimental condition for observing spontaneous photons on dark background with angular and temporal lag from the laser firing. The details of the signal may be varied from one molecular system to another, but the broad conclusion is quite robust.

## Acknowledgments

The work is supported in part by RFBR. AGR thanks Prof. A.Giusti-Suzor and Dr. M.Macholm for the preprint [3] and useful discussions.

## References

- [1] U.Marvet, M.Dantus, "Femtosecond photoassociation spectroscopy: coherent bond formation", *Femtochemistry: Ultrafast Physical and Chemical Processes in Molecular Systems*, M. Chergui ed., p.135, World Scientific, Singapore, 1996.
- [2] E.D.Potter, J.L.Herek, S.Pedersen, Q.Lui and H.Zewail, "Femtosecond laser control of a chemical reaction", *Nature*, **355**, 66, 1992.
- [3] M.Macholm, A.Giusti-Suzor and F.H.Mies, "Photoassociation of atoms in ultracold collisions probed by wave-packet dynamics", *Phys. Rev.*, **A50**, 1994.
- [4] M.T. Zanni, T.R. Taylor, B.J.Greenblatt, B. Soep, and D. M. Neumark "Characterization of the I<sub>2</sub><sup>-</sup> anion ground state using conventional and femtosecond photoelectron spectroscopy," *J. Chem. Phys.*, **107**, 1997; C.Jouviet, M.Boniveau, H.Duval, B.Soep, *J. Phys. Chem.*, **91**, 5416-5422, 1987.
- [5] R.Naplitano, J.Weiner, P.S.Julienne, and C.J.Williams, "Line shapes of high resolution photoassociation spectra of optically cooled atoms", *Phys. Rev. Lett.*, **73**, 1352, 1994.
- [6] P.R.Brooks, "Spectroscopy of transition region species", *Chem. Rev.*, **88**, pp.407-428, 1988.
- [7] P.S.Julienne, "Cold binary atomic collisions in a light field", *J. Res. Nat. Inst. Stand. Technol.*, **101**, 487, 1996; X. T. Wang, H. Wang, P. L. Gould, W. C. Stwalley, E. Tiesinga and P. S. Julienne, "First observation of the pure long-range 1u state of an alkali dimer by photoassociative spectroscopy", *Phys. Rev.*, **A57**, 4600, 1998.
- [8] M.Polanyi, G.Schay, "Über hochverdünnte Flammen III", *Z. Phys. Chem*, **B1**, 30, 1928.
- [9] A.G.Rudavets and I.V.Yevseyev, "Photon echo of molecular photodissociation", *Las. Phys.*, **3** 523-529, 1993.
- [10] V.M.Akulin, V.A.Dubovitskii, A.M.Dykhne, A.G. Rudavets, "Coherent evolution of quantum phase space distribution and photon echo of bound-free transitions", *Femtochemistry: Ultrafast Physical and Chemical Processes in Molecular Systems*, M. Chergui, ed., pp.62-72, World Scientific, Singapore, 1995.
- [11] V.M.Akulin, V.A.Dubovitskii, A.M.Dykhne, A.G. Rudavets, "Laser control of atomic motions insides diatomic molecules", *J. Phys. Chem.*, **A102**(23), pp. 4310-4320, 1998.
- [12] S.Stenholm, K.-A.Suominen, "Weisskopf-Wigner decay of excited oscillator states", *Opt. Exp.*, **2**, p.378, 1998.
- [13] R.Friedberg, S.R.Hartmann, "Billard balls matter-wave interferometry", *Phys. Rev.*, **A48**, pp.1446-1471, 1993.
- [14] E. U. Condon, "Nuclear motions associated with electron transitions in diatomic molecules", *Phys. Rev.*, **32**, pp. 858-872, 1928.
- [15] A.G.Rudavets and M.G.Rudavets, "Thermal spectra of bound-free transitions", *Las. Phys.*, **2**, pp. 523-529, 1992.
- [16] T.H.Dunning, P.J.Hay,"The covalent and ionic states of rare-gas monofluorides" *J. Chem. Phys.*, **69**, 137, 1978; R.B.Jones, J.H.Schloss and J.H.Eden, "Excitation spectra for photoassociation of KrF and X-I collision pairs in the ultraviolet(208-258 nm)", *J. Chem. Phys.*, **98**, 4317, 1993.
- [17] A.I.Krylov, R.B.Gerber, V.A.Apkarian, "Adiabatic approximation and non-adiabatic effects for open-shell atoms in an inert solvent: F atoms in solid Kr", *Chem. Phys.*, **189**, 261-272, 1994.